

EXPERIMENTAL CHARACTERIZATION OF SHIL'NIKOV CHAOS BY STATISTICS OF RETURN  
TIMES

F.T. ARECCHI(\*), A. LAPUCCI(\*), R. MEUCCI(\*), J.A. ROVERSI(\*\*)  
and P.H. COULLET(\*\*\*)

(\*) Istituto Nazionale di Ottica, Largo E. Fermi, 6, 50125 Firenze, Italy

(\*\*) Universidade Estadual de Campinas, Campinas, S.P., Brazil

(\*\*\*) CNRS, Université de Nice, Nice, France

The dynamic behavior of a single-mode  $\text{CO}_2$  laser with feedback is characterized by global features in the phase space, related to the presence of three coexisting unstable fixed points. As a control parameter is monotonically increased, one can observe transitions from a Hopf bifurcation to a local chaos and eventually to regular spiking and Shil'nikov chaos. Furthermore, one can find evidence of competition among these different kinds of instability.<sup>1</sup> The phase-space trajectories are affected differently by each of the three unstable points, and by adjustment of the control parameters they can be characterized by the dominant role of only one, or a pair of them.

A linear stability analysis shows the local features at each fixed point. Precisely, point 0 (at zero intensity) is a saddle node with two stable directions and one unstable; point 1 has a plane unstable manifold with a focus and a stable third direction; point 2 has a stable manifold with a focus and an unstable third direction. Shil'nikov chaos is related to the saddle focus character of point 2. Around a saddle focus the motion consists of a contracting spiral  $\exp(-\lambda t)\cos(\omega t)$  on the stable manifold and of an exponential expansion  $\exp(\gamma t)$  along the unstable manifold. The presence of the other two unstable points ensures that the diverging flow is reinjected into the neighborhood of the saddle focus. Shil'nikov showed that for  $|\lambda| < \gamma$  there exists<sup>2</sup> a countable set of unstable trajectories close to the homoclinic one. This structure of the flow is one of the simplest capable of generating chaotic behavior<sup>3</sup> in many autonomous systems, such as the Lorenz equations<sup>3</sup> and the Belousov-Zhabotinski reaction.<sup>4</sup>

The temporal behavior of laser output intensity in this regime is characterized by pulses almost equal in shape but with chaotic recurrence times.<sup>5</sup> The regularity in shape means that the points at any Poincaré section are so closely packed that impossibly precise measurements of their position would be required if the relevant features of the motion were to be found. Instead, there is a large spread in the return times to

a Poincaré section close to the unstable point. For this reason, the statistics of the return times appears to be the most appropriate characterization of Shil'nikov chaos.<sup>5</sup>

Our experimental setup consists of a single mode CO<sub>2</sub> laser with an intracavity electro-optic modulator. A signal proportional to the laser output intensity is sent back to the electro-optic modulator<sup>6</sup>. Single mode CO<sub>2</sub> lasers have a dynamic behavior described by two coupled differential equations, one for the field amplitude and the other for the population inversion, the fast polarization being adiabatically eliminated from the complete set of Maxwell-Bloch equations.<sup>7</sup> Thus, the presence of feedback introduces a third degree of freedom. When the feedback loop is so fast that it provides a practically instantly adapted loss coefficient, it does not modify the phase-space topology. On other hand, if the time scale of the feedback loop is of the same order as of the other two relevant variables, the system becomes three dimensional. With suitable normalizations such a system is described by three first-order differential equations for the laser intensity  $x(t)$ , the population inversion  $y(t)$ , and the modulation voltage  $z(t)$  as follows:

$$x = -K_x x [1 + \alpha \sin^2(z) - y], \quad (1)$$

$$y = -\gamma_y (y + xy - A), \quad (2)$$

$$z = -\beta (z - B + r x), \quad (3)$$

For a fixed pump  $A$  (fixed discharge current in the laser tube), our system has two control parameters: the bias voltage  $B$  applied to the electro-optic modulator and the gain  $r$  in the feedback loop.

From an experimental point of view we are able to visualize  $(x - z)$  phase-space projections, obtained by feeding onto a scope the photodetector signal proportional to the laser output intensity  $x(t)$  and the feedback voltage  $z(t)$ . These phase-space projections consist of closed orbits visiting successively the neighborhoods of the three unstable stationary points 0, 1, and 2. The local chaos around point 1, established at the end of a subharmonic sequence, has been characterized by standard<sup>6</sup> methods as power spectra and correlation dimension measurements.

However, the existence of a global behavior characterized by pulses with regular shapes but chaotic in their time of occurrence makes it significant to study the dynamics through measurements of return times to a Poincaré section. The measurements have been done by using a threshold circuit. An appropriate Poincaré section  $x = \text{constant}$  can be selected by adjusting the threshold level. This method permits us to distinguish among the different dynamical regimes. Adjusting the control parameters in order to have a dominance of the saddle focus 2, we obtain a motion consisting of a quasi-homoclinic orbit asymptotic to it (Fig. 1). In this regime, the laser output is characterized by pulses with regular shapes but chaotic in their recurrence. Based on such a consideration the iteration map of return times ( $\tau_{i+1}$  versus  $\tau_i$ ) displays an extremely regular structure that we show below to be in close agreement with that arising from Shil'nikov theory of homoclinic chaos.

From a theoretical point of view, a homoclinic orbit asymptotic to a saddle focus<sup>8</sup> can be modeled in terms of the following one-dimensional iteration map:

$$\zeta_{n+1} = \zeta_n^{\lambda/\gamma} \cos[\omega/\gamma \ln(\zeta_n)] + \epsilon, \quad (4)$$

where  $\lambda$  and  $-\lambda \pm i\omega$  are the eigenvalues of the linearized flow at the saddle focus,  $\zeta$  is the coordinate along the unstable manifold, and  $\xi$  is the deviation along  $\zeta$  from the homoclinic orbit at the Poincaré section in the neighborhood of the saddle point ( $\xi = 0$  corresponds to the homoclinic condition).

If we build a small cubic box of unit side centered at the saddle focus and oriented along the eigenvectors  $\xi$ ,  $\eta$ , and  $\zeta$ , any tiny difference in the entrance coordinate along the expanding axis  $\zeta$  will strongly influence the residence time inside the box and hence the spacing from the next reinjection.

Observing that most of the time is spent in the box around the saddle point, we relate the return time  $\tau$  to the coordinate  $\zeta$  of the unstable manifold by  $\zeta = \zeta_0 \exp(\lambda \tau)$ , thus obtaining an iteration map for the return times

$$\begin{aligned} \tau_{n+1} &= -\ln[\exp(-\lambda/\gamma \tau_n) \cos(\omega/\gamma \tau_n) + \epsilon] \\ &= -\ln[\varphi(\tau) + \epsilon], \end{aligned} \quad (5)$$

Comparison of Eqs.(4) and (5) shows the enhanced sensitivity to fluctuations of the  $\tau$  map with respect to the  $\zeta$  map.

Indeed, suppose that the offset  $\delta \xi$  from homoclinicity is affected by a small amount of noise. The sensitivities of the two maps to such a noise are given, respectively, by  $\partial \zeta / \partial \xi = 1$  and

$$\partial \tau / \partial \epsilon = [\varphi(\tau) + \epsilon]^{-1}. \quad (6)$$

This sensitivity factor acts as a lever arm whenever  $\varphi(\tau) + \epsilon$  becomes very small. Note the following: (1) This is not deterministic chaos; in fact, large fluctuations can be expected even for a regular dynamics, implying a fixed point  $\tau^*$ . (2) It is not associated with the homoclinicity condition  $\xi = 0$ ; in fact, for finite  $\xi$  there may be a  $\tau^*$  such that  $\varphi(\tau^*) + \xi = 0$ .

In figures 2 and 3 we show numerical and experimental iteration maps respectively. Fig. 3 also shows the spread related to the enhanced sensitivity to fluctuations.

To summarize, a  $\text{CO}_2$  laser with feedback shows different dynamic regimes depending on the dominant role of one or two of three coexisting unstable stationary points. In particular, in the regime of Shil'nikov chaos the iteration maps of return times display a statistical spread owing to a transient fluctuation enhancement phenomenon peculiar to macroscopic systems, which is absent in low-dimensional chaotic dynamics.

In fact, the model description  $\dot{x} = F(x)$  of a large system in terms of a low-dimensional dynamic variable  $x$  is just an ensemble-averaged description, and residual fluctuations on position  $x$  must be considered at some initial time, even though the successive evolution is accounted for by a deterministic law. In our case such a fluctuation is a stochastic spread  $\delta \xi$  on the offset  $\xi$  of the position  $\zeta$ .

The same amount of  $\delta\xi$  in Eqs.(4) and (5) leaves the  $\mathcal{S}$  maps unaltered, while it strongly affects the  $\mathcal{T}$  maps, making them appear like the experimental data.

We have thus shown a fundamental difference between a small system, ruled by a few equations, and a large system, in which the corresponding low-dimensional dynamics is a contracted description in terms of macroscopic variables, which are ensemble averages over some initial spread.

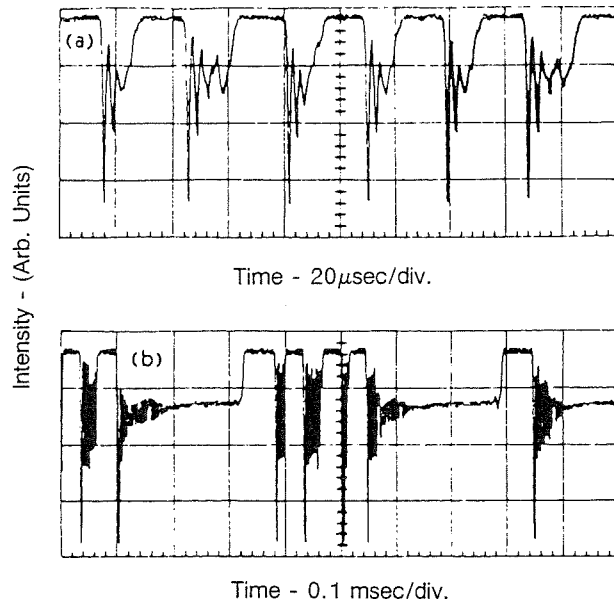


Fig. 1. Time plots of the intensity in the regime of Shil'nikov chaos. (a), (b) Refer to the same B value ( $B = 0.427$ ) but two different gains of the feedback loop. (b) Shows long transients corresponding to a large number of small spirals around the saddle focus.

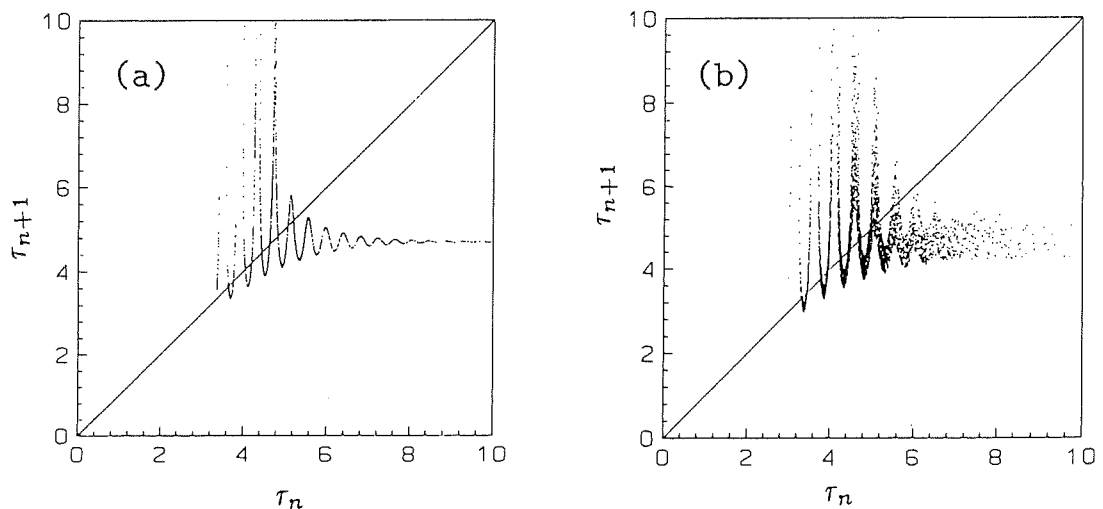


Fig. 2. Numerical iteration maps for Shil'nikov chaos. Parameter values:  $\omega/\gamma = 13.0$ ,  $\alpha/\gamma = 0.986$ ,  $\xi = 0.01$ . (a) and (b),  $\mathcal{T}$  maps without and with noise  $\delta\xi = 10^{-2}$ , respectively.

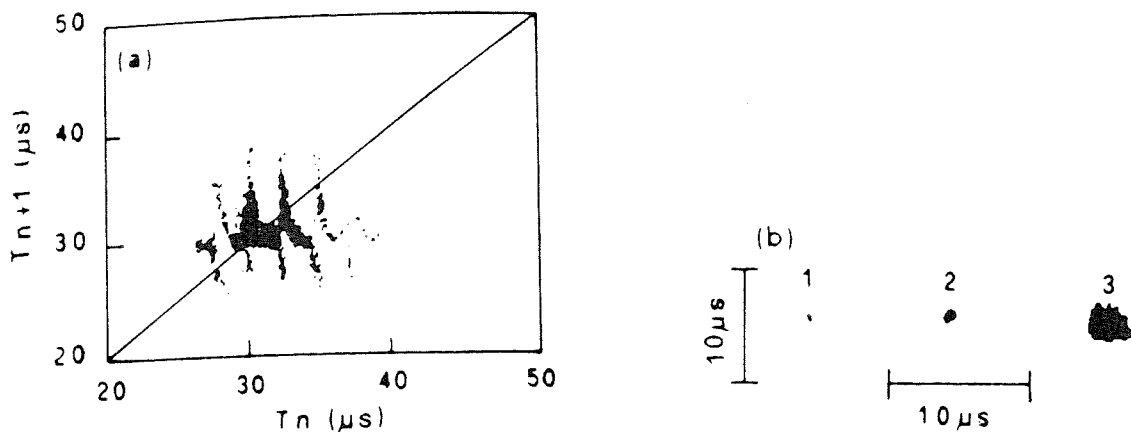


Fig. 3. Experimental iteration maps of the return times. (a)  $r = 0.487$  and  $B = 0.350$ . (b) Maps corresponding to regular periodic situations, namely, 1, an electronic oscillator; 2, the laser in a regular periodic regime; 3, the laser just at the onset of the instability but still with a regular period.

#### REFERENCES

1. F.T. Arecchi, R. Meucci, and W. Gadomski, *Phys Rev. Lett.* **58**, 2205 (1987).
2. L.P. Shil'nikov, *Dokl. Akad. Nauk SSSR* **160**, 558 (1965); L.P. Shil'nikov, *Mat. Sb.* **77**, 119, 461 (1968); **81**, 92, 1213 (1970).
3. P. Glendinning and C. Sparrow, *J. Stat. Phys.* **35**, 645 (1984); P. Gaspard, R. Kapral and G. Nicolis, *J. Stat. Phys.* **35**, 697 (1984).
4. F. Argoul, A. Arneodo, and P. Richetti, *Phys. Lett. A* **120**, 269 (1987).
5. F.T. Arecchi, A. Lapucci, R. Meucci, J.A. Roversi and P. Couillet, *Europhys. Lett.* **6**, 677 (1988).
6. F.T. Arecchi, W. Gadomski and R. Meucci, *Phys. Rev. A* **34**, 1617 (1986).
7. F.T. Arecchi, in "Instabilities and Chaos in Quantum Optics", F.T. Arecchi and R.G. Harrison, eds., Vol. 34 of Springer Series in Synergetics (Springer-Verlag, Berlin, 1987), p. 9.
8. A. Arneodo, P.H. Couillet, E.A. Spiegel and C. Tresser, *Physica* **14D**, 327 (1985).